Liver Diffusion-weighted MR Imaging: Reproducibility Comparison of ADC Measurements Obtained with Multiple Breath-hold, Free-breathing, Respiratory-triggered, and Navigator-triggered Techniques[1]

Xin Chen, MD
Lei Qin, PhD
Dan Pan, MD
Yanqi Huang, MD
Lifen Yan, MD
Guangyi Wang, MD
Yubao Liu, MD, PhD
Changhong Liang, MD, PhD
Zaiyi Liu, MD, PhD

Purpose: To prospectively compare the reproducibility of normal liver apparent diffusion coefficient (ADC) measurements by using different respiratory motion compensation techniques with multiple breath-hold (MBH), free-breathing (FB), respiratory-triggered (RT), and navigator-triggered (NT) diffusion-weighted (DW) imaging and to compare the ADCs at different liver anatomic locations.

Materials and Methods: The study protocol was approved by the institutional review board, and written informed consent was obtained from each participant. Thirty-nine volunteers underwent liver DW imaging twice. Imaging was performed with a 1.5-T MR imager with MBH, FB, RT, and NT techniques (b = 0, 100, and 500 sec/mm^2). Three representative sections—superior, central, and inferior—were selected on left and right liver lobes, respectively. On each selected section, three regions of interest were drawn, and ADCs were measured. Analysis of variance was used to assess ADCs among the four techniques and various anatomic locations. Reproducibility of ADCs was assessed with the Bland-Altman method.

Results: ADCs obtained with MBH (range: right lobe, [1.641–1.662] × 10^{-3}mm^2/sec; left lobe, [2.034–2.054] × 10^{-3}mm^2/sec) were higher than those obtained with FB (right, [1.349–1.391] × 10^{-3}mm^2/sec; left, [1.630–1.700] × 10^{-3}mm^2/sec), RT (right, [1.439–1.455] × 10^{-3}mm^2/sec; left, [1.720–1.755] × 10^{-3}mm^2/sec), or NT (right, [1.387–1.400] × 10^{-3}mm^2/sec; left, [1.661–1.736] × 10^{-3}mm^2/sec) techniques ($P < .001$); however, no significant difference was observed between ADCs obtained with FB, RT, and NT techniques ($P = .130$ to $P > .99$). ADCs showed a trend to decrease moving from left to right. Reproducibility in the left liver lobe was inferior to that in the right, and the central middle segment in the right lobe had the most reproducible ADC. Statistical differences in ADCs were observed in the left-right direction in the right lobe ($P < .001$), but they were not observed in the superior-inferior direction ($P = .144$–$.450$). However, in the left liver lobe, statistical differences existed in both directions ($P = .001$ to $P = .016$ in the left-right direction, $P < .001$ in the superior-inferior direction).

Conclusion: Both anatomic location and DW imaging technique influence liver ADC measurements and their reproducibility. FB DW imaging is recommended for liver DW imaging because of its good reproducibility and shorter acquisition time compared with that of MBH, RT, and NT techniques.

[1] From the Department of Radiology, Guangdong General Hospital, Guangdong Academy of Medical Sciences, 106 Zhongshan Er Road, Guangzhou 510080, China (X.C., D.P., Y.H., L.Y., G.W., Y.L., C.L., Z.L.); Graduate College, Southern Medical University, Guangzhou, China (X.C., D.P.); and Department of Radiology, Dana-Farber Cancer Institute, Boston, Mass (L.Q.). Received July 7, 2013; revision requested August 20; revision received August 26; accepted September 23; final version accepted October 22. Supported by the National Natural Scientific Foundation of China (grant no. 81271569 and 81271654). **Address correspondence to** Z.L. (e-mail: *zyliu@163.com*).

Advances in magnetic resonance (MR) imaging technology have led to increased use of diffusion-weighted (DW) imaging in the detection and characterization of liver lesions (1–4). The apparent diffusion coefficient (ADC) represents mobility of water molecules within tissue and is therefore believed to reflect changes in lesion cellularity and development of microscopic tumor necrosis that can happen before these changes become visible on conventional anatomic images (5–7). Many studies have shown that ADC measurements are helpful in differentiating benign from malignant hepatic lesions and that they can be used as imaging biomarkers in the assessment of treatment response (7–12).

However, ADCs are influenced by many factors, such as image signal-to-noise ratio and motion and susceptibility artifacts (13–15). For liver DW imaging, one of the most important factors is liver motion caused by respiration (15,16). To deal with this factor, four approaches are widely used; these are multiple breath-hold (MBH), free-breathing (FB), respiratory-triggered (RT), and navigator-triggered (NT) DW imaging (16,17). However, little is known of their reproducibility, even though many studies have shown the feasibility of using ADCs measured with MBH, FB, RT, or NT techniques to evaluate liver lesions (15,16,18). To our knowledge, only a few studies (17,19,20) have been performed to compare liver ADC reproducibility measured with the four methods, and the conclusions were not in concordance.

Besides imaging techniques, liver anatomic locations also were shown to affect ADCs (9,19,21). Studies showed that liver parenchyma in segment II had a higher ADC than did liver parenchyma in any other segment and that reproducibility was better in the right lobe than in the left lobe (9,21). It has been shown that cardiac motion is the reason for liver ADC variation; however, the extent to which cardiac motion affects the ADCs in different liver anatomic locations is still unknown. Thus, the purpose of this prospective study was to compare the reproducibility of normal liver ADC measurements by using different respiratory motion compensation techniques with MBH, FB, RT, and NT DW imaging and to compare the ADC values at different liver anatomic locations.

Advances in Knowledge

- Both the diffusion-weighted (DW) imaging acquisition methods and the liver anatomic locations influence the apparent diffusion coefficient (ADC) measurements and their reproducibility.
- Free-breathing (FB) (limits of agreement [LOA]: right lobe, 0.350–0.450; left lobe, 0.425–0.675), respiratory-triggered (RT) (LOA: right, 0.285–0.435; left, 0.360–0.810), and navigator-triggered (NT) (LOA: right, 0.325–0.440; left, 0.395–0.630) DW imaging techniques are more reproducible than is the multiple breath-hold (MBH) technique (LOA: right, 0.365–0.640; left, 0.590–1.090) for liver ADC measurements.
- FB (range: right, [1.349–1.391] $\times 10^{-3}$mm^2/sec, left, [1.630–1.700] $\times 10^{-3}$mm^2/sec), RT (range: right, [1.439–1.455] $\times 10^{-3}$mm^2/sec; left, [1.720–1.755] $\times 10^{-3}$mm^2/sec), and NT (range: right, [1.387–1.400] $\times 10^{-3}$mm^2/sec; left, [1.661–1.736] $\times 10^{-3}$mm^2/sec) DW imaging techniques generate similar mean ADC values, which are significantly lower than those generated with the MBH technique (range: right, [1.641–1.662] $\times 10^{-3}$mm^2/sec; left, [2.034–2.054] $\times 10^{-3}$mm^2/sec).

Implication for Patient Care

- In terms of ADC measurement in the normal liver, free-breathing DW imaging is recommended because of its good reproducibility and shorter acquisition time compared with that of MBH, RT, and NT DW imaging.

Materials and Methods

Study Population

This prospective study was approved by the research ethics committee of Guangdong General Hospital, Guangdong Academy of Medical Sciences, and written informed consent was obtained from each participant. Forty-seven healthy volunteers were referred for MR imaging of the liver between August 2012 and November 2012. The inclusion criteria for this study were as follows: *(a)* no history of drug abuse, viral hepatitis, alcohol abuse, or abdominal surgery, and no current medication use during the study; *(b)* normal appearance of the liver at ultrasonography (no focal or diffuse liver disease, including mild steatosis); and *(c)* ability of the subject to hold his or her breath for up to 20 seconds. The exclusion criteria included *(a)* a history of or findings related to liver disease and contraindications to MR imaging, *(b)* inability of the patient to hold his or her breath for

Published online before print
10.1148/radiol.13131572 **Content codes:** GI MR

Radiology 2014; 271:113–125

Abbreviations:
ADC = apparent diffusion coefficient
DW = diffusion weighted
FB = free breathing
ICC = interclass correlation coefficient
LOA = limits of agreement
MBH = multiple breath hold
NT = navigator triggered
ROI = region of interest
RT = respiratory triggered

Author contributions:
Guarantors of integrity of entire study, all authors; study concepts/study design or data acquisition or data analysis/interpretation, all authors; manuscript drafting or manuscript revision for important intellectual content, all authors; approval of final version of submitted manuscript, all authors; literature research, X.C., L.Q., Y.H., L.Y., Y.L., C.L., Z.L.; clinical studies, X.C., L.Q., D.P., L.Y., G.W., Y.L., Z.L.; statistical analysis, X.C., D.P., G.W., C.L., Z.L.; and manuscript editing, X.C., L.Q., C.L., Z.L.

Conflicts of interest are listed at the end of this article.

up to 20 seconds during DW imaging, *(c)* failure to complete the DW imaging procedure for any reason, and *(d)* poor image quality that was insufficient for image analysis.

MR Imaging Protocol

All volunteers were examined with a 1.5-T MR imager (Magnetom Espree; Siemens Medical Solutions, Erlangen, Germany) with a dedicated six-channel body matrix coil and a 12-channel spine coil. End-expiratory MBH (four breath holds), FB, RT (with an air-filled pressure sensor capable of measuring respiratory-induced pressure changes fixed to the hypochondrial region via a respiration belt around the volunteer), and NT (with a 100-mm-long pencil-beam excitation prepulse at the interface between the liver and lung to detect the position of the right diaphragm) single-shot echo-planar DW imaging examinations were performed in the axial view with three *b* values (0, 100, and 500 sec/mm^2). Fat suppression was achieved with spectral adiabatic inversion recovery (Table 1). Each volunteer was removed from the imager for approximately 15 minutes and then placed inside the imager again for a second DW imaging series. The same imaging parameters were used for the repeated DW imaging series. In total, each volunteer underwent eight DW imaging passes.

Image Analysis

MR images were transferred to a workstation (Viewforum iMAC; Apple, Cupertino, Calif) for postprocessing. ADC maps were calculated by monoexponentially fitting the three *b* value data points with the following equation: $\ln(S) = -b\cdot\mathrm{ADC}+\ln(S_0)$, where S was the signal intensity, b was equal to 100 and 500 sec/mm^2, and S_0 was the signal intensity at a b value of 0 sec/mm^2. The curve fitting used the linear least-squares method to find the optimum ADC that minimizes the summed square of the residuals. The algorithm was developed in house by using Matlab, version 7.7, software (Mathworks, Natick, Mass).

ADCs were measured with ImageJ software (National Institutes of Health, Bethesda, Md) by two radiologists working independently (X.C., D.P.; readers 1 and 2 with 5 and 3 years of clinical experience in liver MR imaging, respectively). Reader 1 measured ADCs twice in a 1-week period; he followed the same procedure to assess intraobserver reproducibility, and his first measurement was compared with the measurement obtained by reader 2 to assess interobserver agreement.

The right and left liver lobes were divided by using the middle hepatic vein as a reference, and ADCs were evaluated separately. Three representative sections were selected for each DW imaging data set. For the right liver lobe (Fig 1a), the central section was obtained through the level of right portal vein, and the superior and inferior sections were obtained three or four section levels above or below the central section, depending on the section thickness (three sections for MBH, four sections for FB, RT, and NT). For the left liver lobe (Fig 1b), the central three continuous sections were selected.

Three equally spaced circular regions of interest (ROIs) each measuring 80 mm^2 were placed in the left and right liver lobes, respectively, in all three selected sections (Fig 1c). All 18 ROIs were placed in the homogeneous liver parenchyma (visible vascular and biliary structures were excluded), with a margin of at least 5 mm from the liver border. For the repeated DW imaging series, ROIs were placed in areas as

Table 1

Imaging Parameters for MBH, FB, RT, and NT MR DW Imaging

Parameter	MBH	FB	RT	NT
Field of view (mm)	350 × 240–280	350 × 240–280	350 × 240–280	350 × 240–280
Matrix	144 × 192	144 × 192	144 × 192	144 × 192
Receiver bandwidth (Hz/pixel)	1302	1302	1302	1302
Repetition time (msec)	800	3800	1500–2000	3800
Echo time (msec)	91	94	94	94
Parallel imaging factor*	2	2	2	2
Section thickness (mm)	7	5.5	5.5	5.5
Intersection gap (mm)	4.9	4.7	4.7	4.7
Acquisition time range (min)†	1–2	2–3	4–6	4–6
No. of signals acquired	2	4	4	4
b value (sec/mm^2)	0, 100, 500	0, 100, 500	0, 100, 500	0, 100, 500
No. of sections per stack	17	17	17	17
Echo spacing (msec)	0.95	0.95	0.95	0.95
Fat suppression	SPAIR	SPAIR	SPAIR	SPAIR

Note.— SPAIR = spectral adiabatic inversion recovery.

* Performed by using a k-space–based technique (GRAPPA; Siemens Medical Solutions).

† Variable depended on respiratory cycle and interacquisition interval in MBH.

Figure 1

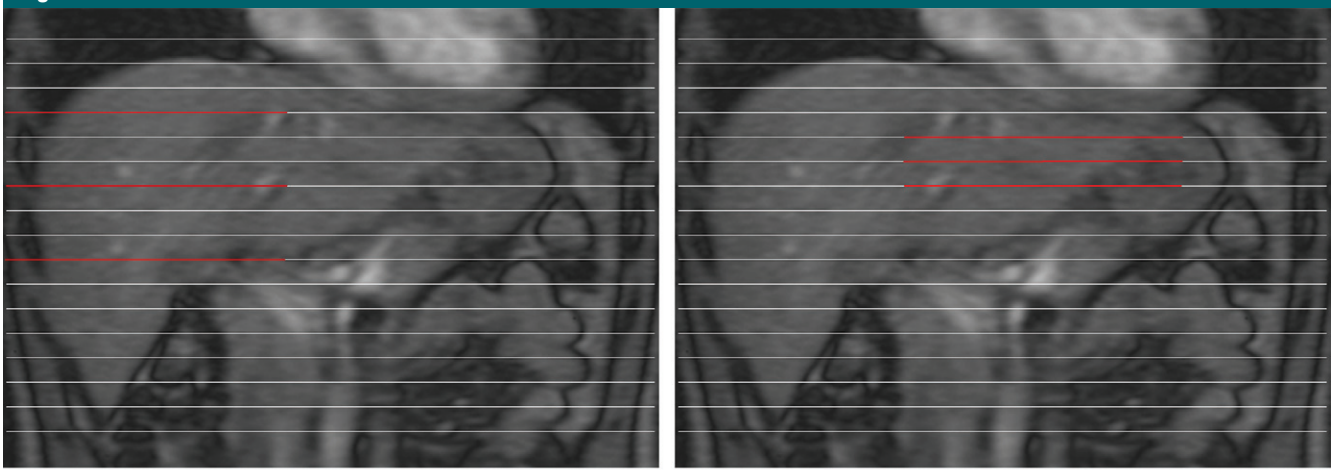

a. b.

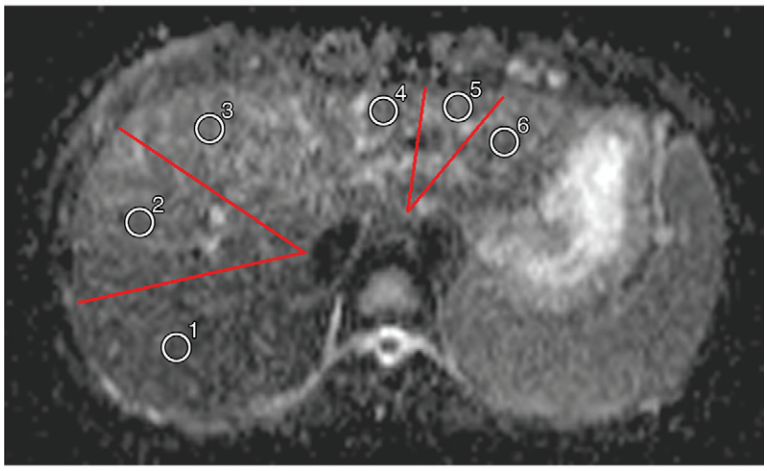

c.

Figure 1: Diagrams show ROI placement. **(a, b)** Red lines are the three selected sections of the **(a)** right and **(b)** left liver lobes for ADC measurements. **(c)** ROIs 1, 2, and 3 represent the three ROIs in the right, middle, and left segments of the right lobe, respectively. ROIs 4, 5, and 6 represent the three ROIs in the right, middle, and left segments of the left lobe, respectively.

similar to one another as possible; this was achieved visually by using anatomic landmarks, such as the main portal vein and its right branches in the liver.

Thus, a total of 144 ADCs were collected for each volunteer (two repeated series, three sections per lobe, two lobes, three ROIs per lobe per section, and four techniques).

Statistical Analysis

The sample size was determined by using power analysis according to our pretest values between two repeated examinations for each technique by presuming an expected difference of 0, an allocation ratio of 1, an α value of .05, and a power of 0.9, yielding an expected sample size of 36. We enrolled a total of 46 subjects, assuming a failure rate of about 25% for the possibility of unpredictable events, such as poor image quality or incomplete DW imaging examinations.

ADCs were expressed as mean ± standard deviation and were tested first with the Kolmogorov-Smirnov test for normality and then with the Levene test for variance homogeneity.

Intra- and interobserver agreement of ADC measurements were evaluated by using intra- and interclass correlation coefficients (ICCs) (22,23). The average ADC from all nine ROIs was used for ICC calculation. Intraobserver ICC was computed from reader 1's two measurements. Interobserver ICC was computed from reader 1's first measurements and from reader 2's measurements. An ICC greater than 0.75 was indicative of good agreement (23).

The reproducibility of ADC measurements was evaluated with the Bland-Altman method (24). The mean absolute difference (bias) and the 95% confidence interval of the mean difference (limits of agreement [LOAs]) between the first and second DW imaging series were compared (25). To evaluate the systematic bias of repeated ADC measurements, the average ADC from the nine ROIs in both the right liver lobe and the left liver lobe were compared between the two repeated series by using a paired-sample *t* test for each technique.

Next, for each MBH, FB, RT, and NT DW imaging series, the differences between left and right liver lobes were evaluated by comparing the average ADCs from the nine ROIs in each lobe by using a paired-sample *t* test. The difference between these four techniques was assessed by using two-way classification analysis of variance.

Finally, the difference in ADCs among the nine individual ROIs on each liver lobe was assessed by using three-way classification analysis of variance. The Bonferroni method was used to adjust for multiple comparisons, when necessary.

Statistical analyses were performed by using SPSS (version 19.0; SPSS, Chicago, Ill) and MedCalc (MedCalc, Mariakerke, Belgium) software. Differences were considered significant when *P* values were less than .05.

Results

Population Demographics

Forty-six volunteers were enrolled in this study. Seven of them did not complete the study because of poor image quality due to frequent bulk movement during acquisition (n = 4) or incomplete acquisition of all DW imaging sequences ascribed to long acquisition time (n = 3). Thirty-nine volunteers successfully completed the imaging examinations (15 men, 24 women; mean age, 24 years ± 3; age range, 20–32 years; mean age of men, 25 years ± 2; age range, 22–29 years; mean age of women, 23 years ± 3, age range, 20–32 years).

Intra- and Interobserver Agreement of ADC Measurement

The intraobserver ICC calculated based on reader 1's two measurements ranged from 0.853 to 0.982 (Table 2). The lowest ICC was 0.853, and it came from the MBH examination; the highest ICC was 0.982, and it came from the FB examination. Interobserver agreement between reader 1's first measurements and reader 2's measurements was good for the four techniques, with ICCs ranging from 0.829 to 0.952 (Table 2).

For the intra- and interobserver agreement tests, the FB, RT, and NT techniques offer consistently higher ICC than does the MBH technique.

Reproducibility of ADC Measurements in the Right and Left Liver Lobes with Four Techniques

Overall, ADC reproducibility of the right liver lobe was better than that of the left lobe with any of the four techniques, and FB, RT, and NT techniques were always superior to the MBH technique (Table 3). For instance, the LOA between the two repeated DW imaging examinations in the superior right ROI in the right liver lobe was 0.640 × 10^{-3}mm^2/sec with MBH, 0.395 × 10^{-3}mm^2/sec with FB, 0.315 × 10^{-3}mm^2/sec with RT, and 0.375 × 10^{-3}mm^2/sec with NT, while the LOA in the superior right ROI of the left liver lobe was much higher (MBH, 1.090 × 10^{-3}mm^2/sec; FB, 0.600 × 10^{-3}mm^2/sec; RT, 0.515 × 10^{-3}mm^2/sec; and NT, 0.590 × 10^{-3}mm^2/sec).

In the right liver lobe, reproducibility of ADC measurements of the nine ROIs in different anatomic locations varied for each technique. The LOA was (0.365–0.640) × 10^{-3}mm^2/sec with MBH, (0.325–0.450) × 10^{-3}mm^2/sec with FB, (0.285–0.435) × 10^{-3}mm^2/sec with RT, and (0.325–0.440) × 10^{-3}mm^2/sec with NT. Reproducibility of ADC measurements in the central middle location was superior to that in other anatomic locations for all the techniques, yielding mean absolute differences of ADCs ± LOA of (−0.03 ± 0.365) × 10^{-3}mm^2/sec with MBH, (0.02 ± 0.325) × 10^{-3}mm^2/sec with FB, (−0.02 ± 0.285) × 10^{-3}mm^2/sec with RT, and (−0.04 ± 0.325) × 10^{-3}mm^2/sec with NT (Table 3, Fig 2).

In the left liver lobe, the LOA of all nine ROIs was larger than the LOA of ROIs in the right liver. The LOA was (0.590–1.090) × 10^{-3}mm^2/sec with MBH, (0.425–0.675) × 10^{-3}mm^2/sec with FB, (0.360–0.810) × 10^{-3}mm^2/sec with RT, and (0.395–0.630) × 10^{-3}mm^2/sec with NT. When we took both the mean absolute difference and

Table 2

Intra- and Interobserver Agreement for ADC Measurement

Agreement	MBH		FB		RT		NT	
	First DW Imaging Series	Second DW Imaging Series	First DW Imaging Series	Second DW Imaging Series	First DW Imaging Series	Second DW Imaging Series	First DW Imaging Series	Second DW Imaging Series
Intraobserver	0.853 (0.673, 0.923)	0.891 (0.812, 0.941)	0.963 (0.923, 0.978)	0.982 (0.923, 0.991)	0.923 (0.852, 0.958)	0.972 (0.933, 0.989)	0.954 (0.899, 0.972)	0.897 (0.853, 0.925)
Interobserver	0.829 (0.667, 0.912)	0.881 (0.796, 0.939)	0.952 (0.907, 0.975)	0.943 (0.890, 0.970)	0.926 (0.856, 0.962)	0.932 (0.867, 0.965)	0.881 (0.769, 0.939)	0.913 (0.831, 0.955)

Note.—Data in parentheses are 95% confidence intervals.

Table 3

Reproducibility of ADC Measurement in Each of the Nine Anatomic Locations in the Right and Left Liver Lobes with Four Techniques

Anatomic Location	Right Liver Lobe				Left Liver Lobe			
	MBH ($\times 10^{-3}$ mm^2/sec)	FB ($\times 10^{-3}$ mm^2/sec)	RT ($\times 10^{-3}$ mm^2/sec)	NT ($\times 10^{-3}$ mm^2/sec)	MBH ($\times 10^{-3}$ mm^2/sec)	FB ($\times 10^{-3}$ mm^2/sec)	RT ($\times 10^{-3}$ mm^2/sec)	NT ($\times 10^{-3}$ mm^2/sec)
Superior right	0.02 (0.640)	0.00 (0.395)	0.02 (0.315)	−0.01 (0.375)	−0.08 (1.090)	0.06 (0.600)	0.01 (0.515)	0.04 (0.590)
Superior middle	−0.01 (0.540)	0.03 (0.345)	0.02 (0.325)	0.08 (0.360)	−0.17 (1.050)	0.05 (0.675)	0.08 (0.810)	0.08 (0.570)
Superior left	−0.11 (0.505)	0.03 (0.425)	0.03 (0.395)	0.03 (0.400)	−0.03 (1.090)	0.05 (0.535)	0.02 (0.630)	0.05 (0.540)
Central right	−0.03 (0.465)	0.00 (0.370)	−0.02 (0.325)	0.05 (0.395)	0.02 (0.680)	0.11 (0.425)	−0.01 (0.495)	0.14 (0.395)
Central middle	−0.03 (0.365)	0.02 (0.325)	−0.02 (0.285)	−0.04 (0.325)	−0.08 (0.795)	0.07 (0.520)	−0.03 (0.540)	0.04 (0.535)
Central left	0.06 (0.410)	0.03 (0.450)	0.00 (0.365)	0.03 (0.440)	−0.04 (0.835)	0.14 (0.575)	−0.06 (0.550)	0.06 (0.630)
Inferior right	−0.00 (0.495)	0.00 (0.385)	0.01 (0.370)	0.02 (0.335)	0.01 (0.590)	0.01 (0.425)	−0.02 (0.360)	−0.07 (0.435)
Inferior middle	0.04 (0.455)	0.00 (0.350)	0.00 (0.325)	−0.02 (0.340)	0.14 (0.915)	0.06 (0.565)	0.01 (0.515)	0.07 (0.505)
Inferior left	0.02 (0.470)	0.00 (0.355)	0.03 (0.435)	−0.02 (0.400)	0.05 (0.835)	0.06 (0.562)	0.05 (0.495)	0.04 (0.555)

Note.—Data in parentheses are 95% LOA. *Superior*, *central*, and *inferior* refer to the superior, central, and inferior sections of the liver lobe, respectively. *Right*, *middle*, and *left* refer to the right, middle, and left ROIs, respectively. The central middle ROI in the right liver lobe and the inferior right ROI in the left liver lobe have the best reproducibility.

the LOA into consideration, ADC in the inferior right ROI showed the best reproducibility; this was (0.01 ± 0.590) × 10^{-3}mm^2/sec with MBH, (0.01 ± 0.365) × 10^{-3}mm^2/sec with FB, (0.02 ± 0.360) × 10^{-3}mm^2/sec with RT, and (0.07 ± 0.435) × 10^{-3}mm^2/sec with NT (Table 3, Fig 3).

Mean ADCs in Left and Right Liver Lobes with Four Techniques

Table 4 shows the comparison results of mean ADCs from the nine ROIs in each liver lobe. For both readers, left lobe ADCs were significantly greater than right lobe ADCs with all four techniques ($P < .001$).

ADCs with the MBH technique (right, [1.641–1.662] × 10^{-3}mm^2/sec; left, [2.034–2.054] × 10^{-3}mm^2/sec) were significantly higher than those with the FB (right, [1.349–1.391] × 10^{-3}mm^2/sec; left, [1.630–1.700] × 10^{-3}mm^2/sec), RT (right, [1.439–1.455] × 10^{-3}mm^2/sec; left, [1.720–1.755] × 10^{-3}mm^2/sec), or NT (right, [1.387–1.400] × 10^{-3}mm^2/sec; left, [1.661–1.736] × 10^{-3}mm^2/sec) technique for both readers on both repeated images and for both left and right liver lobes ($P < .001$) (Table 4); however, no significant difference was noticed between FB, RT, and NT techniques ($P = .130$ to $P > .99$).

ADCs of Different Anatomic Liver Locations

Mean ADCs from the two repeated series ± standard deviation of different anatomic liver locations for reader 1 are shown in Table 5. Reader 2's results were similar and are not shown.

For all four techniques, ADCs showed a decreasing trend in the left-right direction (Fig 4). The differences of ADCs in that direction for both left and right liver lobes were all significantly different (right lobe, $P < .001$; left lobe, $P = .001$ to $P = .016$) (Table 5). On the other hand, in the superior-inferior direction, ADCs in the left lobe clearly decreased ($P < .001$) (Fig 4); however, no significant difference was observed in the right lobe ($P = .144$ to $P = .450$). In general, standard deviation of ADCs in the left liver lobe was much

Figure 2

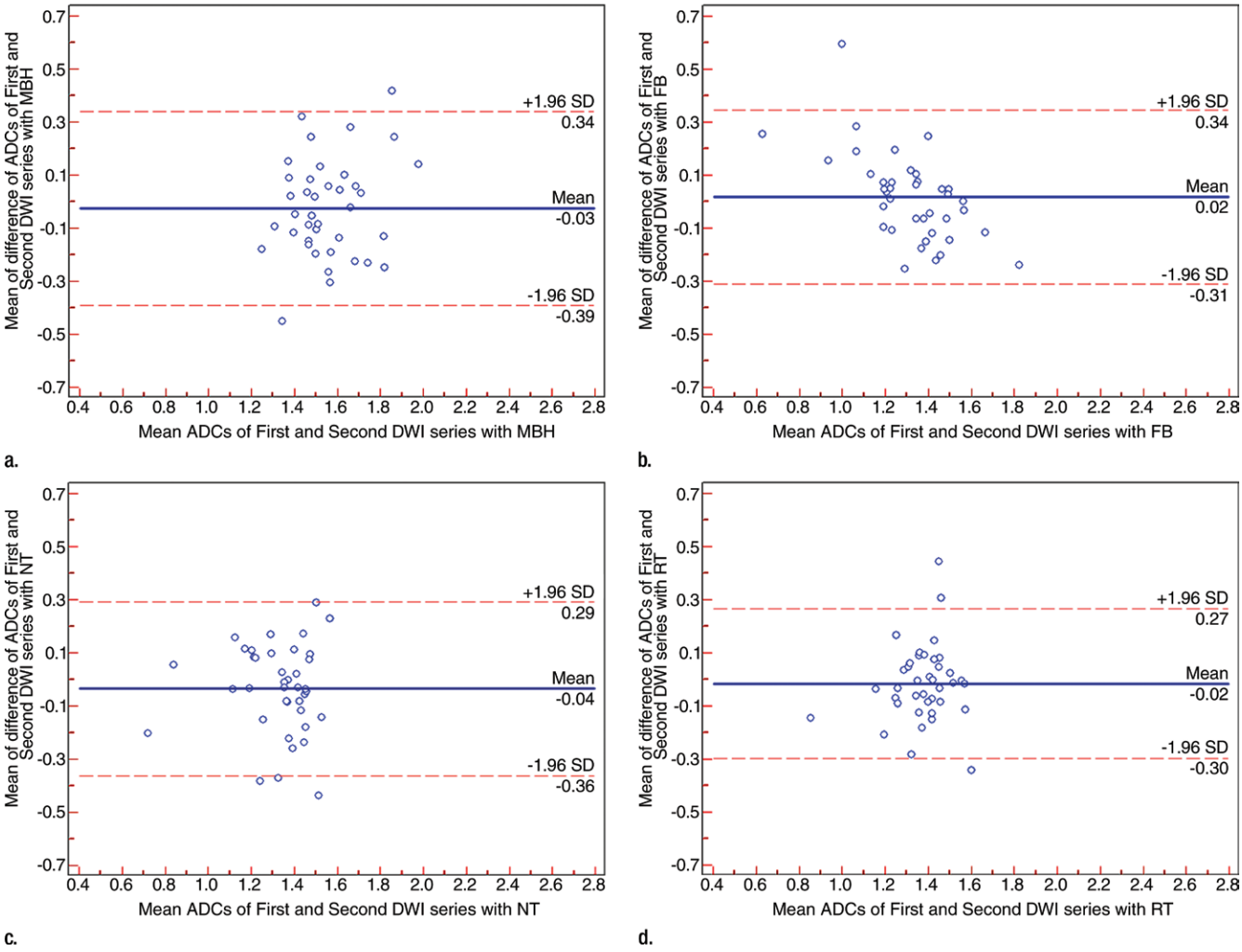

Figure 2: Bland-Altman plots show reproducibility of ADCs ($\times 10^{-3}$ mm^2/sec) in the central middle location of the right liver lobe with four techniques: **(a)** MBH, **(b)** FB, **(c)** NT, and **(d)** RT. Blue line = mean absolute difference, red lines = 95% confidence interval of the mean difference (LOA).

larger than that in the right liver lobe (Fig 4).

Discussion

DW imaging is now widely implemented in clinical practice to detect and characterize liver lesions. Breath-hold DW imaging was routinely used because the liver can be imaged in one to two breath holds of approximately 20 seconds each; however, it suffers from a low signal-to-noise ratio and a low spatial resolution. On the other hand, FB, NT, and RT DW imaging can be performed with multiple excitations to reduce the effects of motion and attain a higher signal-to-noise ratio; however, this comes at the expense of a prolonged acquisition time. Because of the various choices of acquisition techniques and the complexity of motion-inducing unreliable ADC measurements, to our knowledge, no consensus on the optimal liver DW imaging acquisition scheme currently exists.

Several studies have suggested that cardiac motion caused signal loss during liver DW imaging, which resulted in artificially increased ADC (26,27). Kwee et al (26) used dynamic DW imaging to examine the effects of the heart on liver DW images and found that DW images obtained in the systolic phase had lower signal intensity than did DW images obtained in the diastolic phase and that the left liver lobe was more affected than the right. Their findings were in line with our results, which showed that the left liver lobe had significantly higher ADCs and larger LOA than did the right liver lobe. In the superior-inferior direction, ADCs decreased significantly in the left liver lobe but not the right liver lobe, where the cardiac motion effect was expected to be smaller. Furthermore, ADCs showed a clear decreasing trend

Figure 3

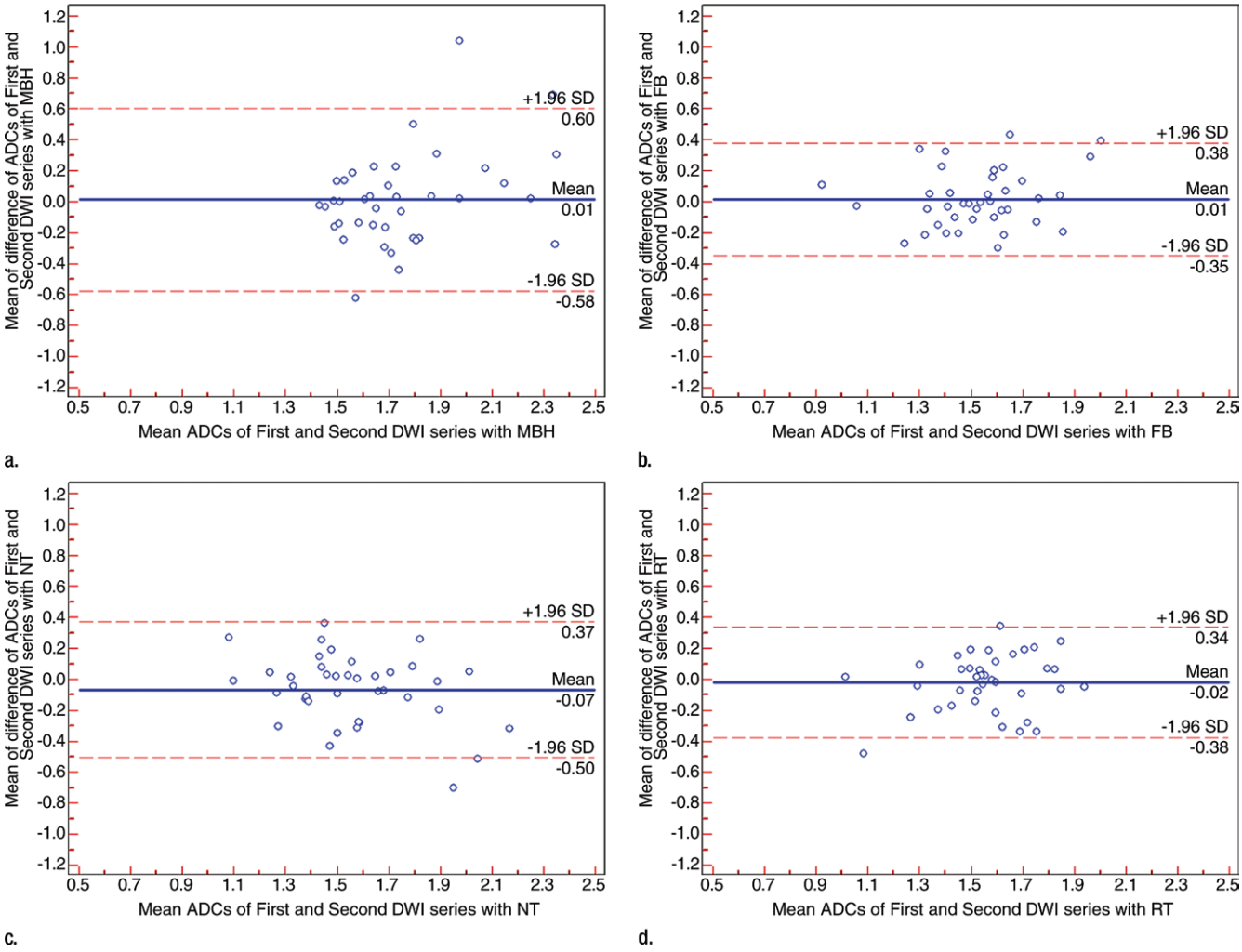

Figure 3: Bland-Altman plots show reproducibility of ADCs ($\times 10^{-3}$ mm^2/sec) in the inferior right location of left lobe with four techniques: **(a)** MBH, **(b)** FB, **(c)** NT, and **(d)** RT. Blue line = mean absolute difference, red lines = 95% confidence interval of the mean difference (LOA).

from left to right (ie, farther from the heart). In the left liver lobe, the most reproducible ADC was measured in the inferior right segment, which was expected because that segment was the farthest from the heart and thus was minimally affected by cardiac motion. If cardiac motion was considered the major source of motion that influenced ADC measurement, the most reproducible ADC measurement in the right liver lobe, theoretically, should be the inferior right segment. However, our results showed that the most reproducible segment was the central middle segment. Thus, there must be other motion affecting ADC measurements in the right liver lobe. One possibility was that the superior segment of the right liver lobe was affected more by cardiac motion, as expected; however, the inferior segment was influenced more by intestinal peristalsis instead, and the right segment was influenced more by abdominal wall and diaphragm motion. However, this hypothesis needs to be confirmed in future studies.

Our results showed that all the LOAs were around 30% of the mean ADC, with the exception of MBH in the left liver lobe (maximum LOA was approximately 50% of the mean ADC); this finding was in agreement with the findings of Kim et al (19). Thus, for treatment response evaluation with ADC as a biomarker, we also recommend a confident threshold to be at least 30%, and the same DW imaging acquisition technique should be used for all baseline and follow-up studies.

Nasu et al (28) showed that signal intensity decrease was less prominent in trace images because average signal intensity was calculated; this finding was in agreement with our results. When we compare MBH (two signals acquired) with FB, NT, and RT (four

Table 4

Mean ADCs of Right and Left Liver Lobes with Four Techniques

Series and Reader	MBH		FB		RT		NT		P Value*
	Right Lobe	Left Lobe	Right Lobe	Left Lobe	Right Lobe	Left Lobe	Right Lobe	Left Lobe	
Reader 1									
First	1.641 ± 0.137	2.034 ± 0.270	1.389 ± 0.139	1.700 ± 0.218	1.447 ± 0.129	1.755 ± 0.211	1.400 ± 0.120	1.736 ± 0.260	<.001
Second	1.662 ± 0.180	2.054 ± 0.265	1.378 ± 0.153	1.632 ± 0.203	1.439 ± 0.123	1.749 ± 0.208	1.387 ± 0.138	1.687 ± 0.209	<.001
Mean	1.653 ± 0.156	2.051 ± 0.247	1.380 ± 0.143	1.660 ± 0.200	1.443 ± 0.121	1.738 ± 0.192	1.398 ± 0.134	1.695 ± 0.168	<.001
P value†	<.001	…	<.001	…	<.001	…	<.001	…	…
Reader 2									
First	1.655 ± 0.205	2.052 ± 0.412	1.391 ± 0.155	1.672 ± 0.273	1.455 ± 0.189	1.720 ± 0.279	1.387 ± 0.178	1.713 ± 0.286	<.001
Second	1.658 ± 0.196	2.054 ± 0.395	1.349 ± 0.171	1.630 ± 0.281	1.445 ± 0.182	1.720 ± 0.278	1.398 ± 0.192	1.661 ± 0.248	<.001
Mean	1.657 ± 0.141	2.053 ± 0.241	1.370 ± 0.131	1.651 ± 0.211	1.450 ± 0.155	1.720 ± 0.202	1.384 ± 0.134	1.693 ± 0.188	<.001
P value†	<.001	…	<.001	…	<.001	…	<.001	…	…

Note.—Data are mean ± standard deviation. *First* = first DW imaging series, *Second* = second DW imaging series.

* Two-way analysis of variance revealed significant differences in ADCs between the right and left liver lobes with MBH, FB, RT, and NT techniques.

† *P* values were obtained by using the paired *t* test to compare differences between the right and left liver lobes for each technique.

signals acquired), ADCs were significantly higher with MBH (ie, more signal intensity decrease) and less reproducible. However, conflicting results were reported previously for comparison of these acquisition techniques. Kwee et al (17) showed the reproducibility of ADC measurements in normal liver parenchyma with breath-holding (two signals acquired) and FB (four or five signals acquired) examinations was comparable to but better than that obtained with an RT examination (two signals acquired) and that ADCs obtained with an RT sequence were significantly larger than those obtained with a BH or FB sequence. The possible reason for the higher and more scattered ADCs with RT DW imaging was the fact that only two excitations were used in the Kwee et al study, and there may have been a mismatch in the end-expiratory diaphragm levels between sequential triggering events. Furthermore, Taouli et al (16) reported more reproducible but significantly higher ADC with the NT technique (four signals acquired) than with the BH technique (two signals acquired). They speculated that the higher ADC with the NT technique might have been due to the improved signal-to-noise ratio from the increased number of signals acquired and the longer repetition time. Kim et al (19,29) also reported a higher ADC in malignant hepatic tumors with the RT technique (four signals acquired) than with the BH technique (two signals acquired). On the contrary, similar to our results, Jerome et al (20) recently compared FB and NT abdominal DW imaging and reported no significant difference between the two acquisition techniques. In that study, the acquisition time was 10 minutes for each technique, within which the FB technique yielded consistently more excitations (5.5 excitations ± 0.2 vs 3.9 excitations ± 0.1). The fewer excitations yielded by NT resulted in poorer confidence in ADC estimation even though NT examinations did indeed reduce the range of motion (6.0 mm ± 1.4 for NT vs 10.0 mm ± 1.7 for FB). The motion range

Table 5

ADCs in Different Anatomic Locations of the Right and Left Liver Lobe with Four Techniques

	Left Liver Lobe				Right Liver Lobe			
	Left	Middle	Right	P Value	Left	Middle	Right	P Value*
MBH								
Superior	2.424 ± 0.586	2.356 ± 0.474	2.038 ± 0.375	<.001	1.720 ± 0.244	1.599 ± 0.198	1.665 ± 0.253	<.001
Central	2.025 ± 0.399	1.955 ± 0.359	1.812 ± 0.281	…	1.620 ± 0.239	1.543 ± 0.208	1.668 ± 0.275	…
Inferior	1.986 ± 0.379	1.949 ± 0.433	1.761 ± 0.340	…	1.725 ± 0.240	1.602 ± 0.191	1.629 ± 0.187	…
P value†	<.001	…	…	…	.190	…	…	…
FB								
Superior	1.904 ± 0.273	1.858 ± 0.315	1.831 ± 0.294	.006	1.598 ± 0.204	1.364 ± 0.159	1.260 ± 0.203	<.001
Central	1.791 ± 0.362	1.660 ± 0.289	1.593 ± 0.231	…	1.553 ± 0.205	1.328 ± 0.244	1.282 ± 0.207	…
Inferior	1.607 ± 0.244	1.501 ± 0.282	1.534 ± 0.252	…	1.541 ± 0.188	1.323 ± 0.174	1.252 ± 0.223	…
P value†	<.001	…	…	…	.405	…	…	…
RT								
Superior	1.965 ± 0.370	2.021 ± 0.416	1.893 ± 0.330	.012	1.597 ± 0.174	1.370 ± 0.159	1.319 ± 0.219	<.001
Central	1.760 ± 0.260	1.679 ± 0.296	1.639 ± 0.243	…	1.565 ± 0.174	1.392 ± 0.222	1.354 ± 0.176	…
Inferior	1.701 ± 0.239	1.589 ± 0.226	1.548 ± 0.233	…	1.600 ± 0.168	1.422 ± 0.230	1.405 ± 0.200	…
P value†	<.001	…	…	…	.144	…	…	…
NT								
Superior	1.929 ± 0.290	1.933 ± 0.295	1.883 ± 0.301	.016	1.584 ± 0.229	1.416 ± 0.183	1.288 ± 0.207	<.001
Central	1.831 ± 0.327	1.662 ± 0.317	1.646 ± 0.258	…	1.540 ± 0.176	1.316 ± 0.192	1.320 ± 0.211	…
Inferior	1.622 ± 0.300	1.590 ± 0.265	1.529 ± 0.238	…	1.520 ± 0.175	1.331 ± 0.227	1.290 ± 0.200	…
P value†	<.001	…	…	…	.153	…	…	…

Note.—Data are mean ± standard deviation. *Left*, *middle*, and *right* refer to the left, middle, and right segments, respectively, of the left and right liver lobes. *Superior*, *central*, and *inferior* refer to superior, central, and inferior sections, respectively, of the right and left liver lobes.

* Comparison of ADCs in the left-right direction.

† Comparison of ADCs in the superior-inferior direction.

Figure 4

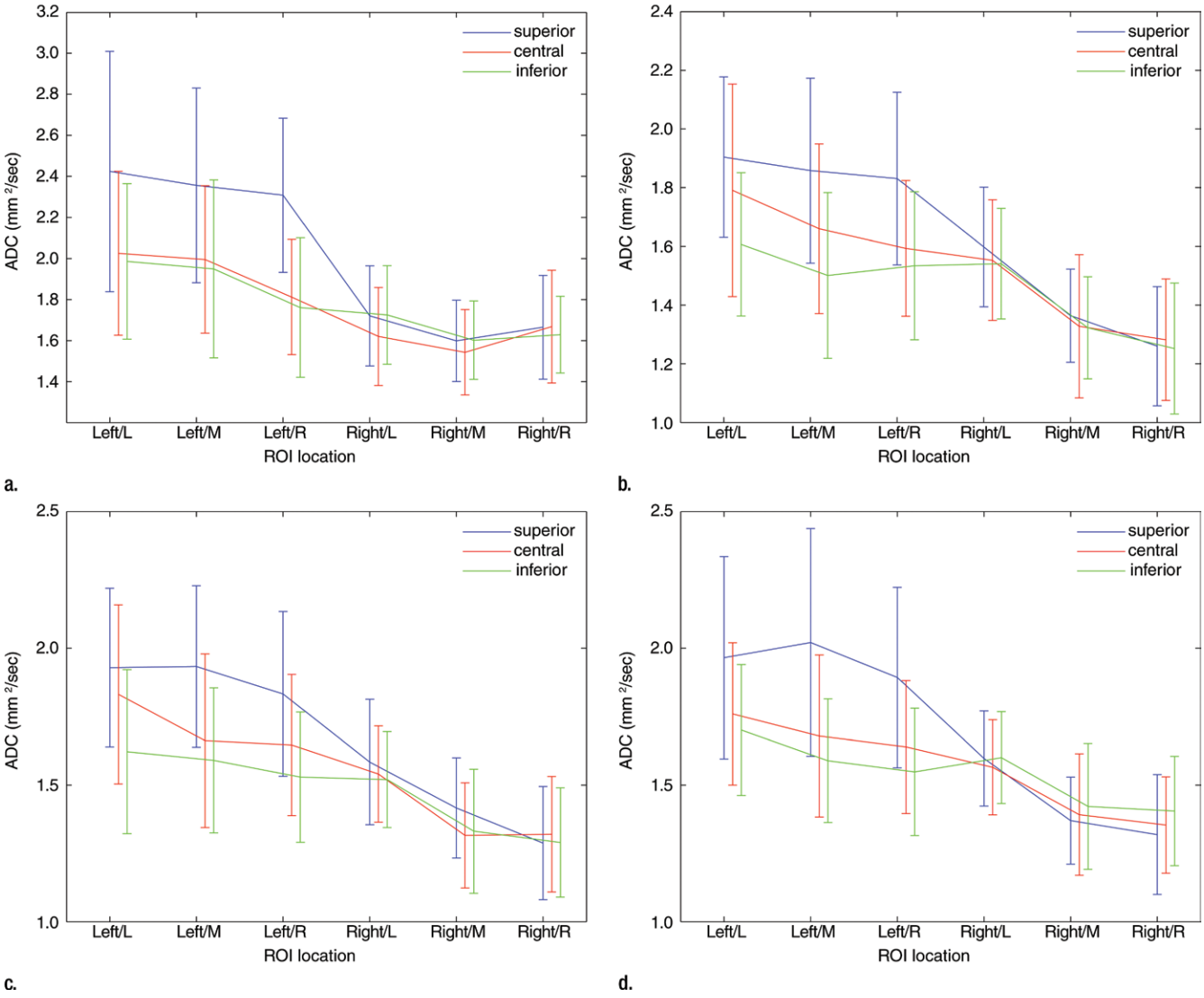

Figure 4: ADCs plots of different liver locations with **(a)** MBH, **(b)** FB, **(c)** NT, and **(d)** RT DW imaging. *Central* = central section of the liver lobes, *inferior* = inferior section of the liver lobes, *L* = left segment of the liver lobe, *left* = left liver lobe, *M* = middle segment of the liver lobe, *R* = right segment of the liver lobe, *Right* = right liver lobe, *superior* = superior section of the liver lobe.

difference between NT and FB examinations surprisingly was not significant, which may explain the comparable ADC measurements observed in their study. They did not test RT DW imaging, but we believe that RT would generate a similar or slightly larger range of motion than NT because the triggering was based on a pressure sensor, which was not as accurate as directly navigator measuring the motion of the diaphragm. This also explained why in our study, with the same number of signals acquired, we obtained similar ADC measurements with FB, NT, and RT. The reason for the discrepancy in ADC values from the previous studies and our current study was not fully understood; however, one consistent finding was that more excitations generated more reproducible ADCs. Thus, even though liver ADC measurements can be affected by cardiac motion, respiratory motion, and hepatic local motion, a reasonable and reproducible ADC can be measured by using more excitations during DW imaging acquisition. More excitations can improve the possibility of DW image acquisition during the diastolic phase that resulted in higher signal intensity as compared with that in the systolic phase (26). Furthermore, acquisition of multiple signals can compensate for signal loss in DW imaging.

Our study had several limitations. First, comparison and assessment of reproducibility of ADC measurements were performed with data from only normal liver parenchyma in a young healthy population. It is important to realize that the results in normal liver and hepatic tumors (hepatic tumors have a more heterogeneous microenvironment), as well as those in young and old populations, may differ. Thus, our reproducibility may be overestimated for a patient population.

Second, the section thickness and number of signals acquired for the MBH technique were different from the section thickness and number of signals acquired for the FB, RT, and NT techniques, which may have caused some bias. However, MBH DW imaging with two signals acquired already required four breath holds. Thus, it was more acceptable for the subject to complete the current MBH DW imaging examination than for him or her to undergo MBH DW imaging with four signals acquired, which would have required eight breath holds and a much longer acquisition time. Furthermore, acquisition of two signals for MBH DW imaging offered sufficient signal-to-noise ratio in our opinion; therefore, we optimized the number of signals acquired as two for the MBH technique.

Finally, in our study, we used three *b* values (0, 100, and 500 sec/mm^2) for ADC measurements. Since the perfusion fraction was not excluded and because only monoexponential fitting was performed, the ADC values might have been overestimated; however the reproducibility should have remained the same.

In conclusion, we recommend that ADC measurement of the liver parenchyma be performed with FB DW imaging in clinical practice and research because of its good reproducibility and shorter acquisition time compared with that of MBH, RT, and NT DW imaging. ADC of the central middle segment in the right lobe has the best reproducibility and should be used as the reference standard when liver ADC is used as a biomarker for clinical applications, such as monitoring treatment responses.

Disclosures of Conflicts of Interest: X.C. No relevant conflicts of interest to disclose. **L.Q.** No relevant conflicts of interest to disclose. **D.P.** No relevant conflicts of interest to disclose. **Y.H.** No relevant conflicts of interest to disclose. **L.Y.** No relevant conflicts of interest to disclose. **G.W.** No relevant conflicts of interest to disclose. **Y.L.** No relevant conflicts of interest to disclose. **C.L.** No relevant conflicts of interest to disclose. **Z.L.** No relevant conflicts of interest to disclose.

References

1. Wagner M, Doblas S, Daire JL, et al. Diffusion-weighted MR imaging for the regional characterization of liver tumors. Radiology 2012;264(2):464–472.
2. Taouli B. Diffusion-weighted MR imaging for liver lesion characterization: a critical look. Radiology 2012;262(2):378–380.
3. Taouli B, Koh DM. Diffusion-weighted MR imaging of the liver. Radiology 2010;254(1):47–66.
4. Soyer P, Corno L, Boudiaf M, et al. Differentiation between cavernous hemangiomas and untreated malignant neoplasms of the liver with free-breathing diffusion-weighted MR imaging: comparison with T2-weighted fast spin-echo MR imaging. Eur J Radiol 2011;80(2):316–324.
5. Nicholson C, Phillips JM. Ion diffusion modified by tortuosity and volume fraction in the extracellular microenvironment of the rat cerebellum. J Physiol 1981;321:225–257.
6. Szafer A, Zhong J, Anderson AW, Gore JC. Diffusion-weighted imaging in tissues: theoretical models. NMR Biomed 1995;8(7-8):289–296.
7. Mannelli L, Kim S, Hajdu CH, Babb JS, Clark TW, Taouli B. Assessment of tumor necrosis of hepatocellular carcinoma after chemoembolization: diffusion-weighted and contrast-enhanced MRI with histopathologic correlation of the explanted liver. AJR Am J Roentgenol 2009;193(4):1044–1052.
8. Parikh T, Drew SJ, Lee VS, et al. Focal liver lesion detection and characterization with diffusion-weighted MR imaging: comparison with standard breath-hold T2-weighted imaging. Radiology 2008;246(3):812–822.
9. Filipe JP, Curvo-Semedo L, Casalta-Lopes J, Marques MC, Caseiro-Alves F. Diffusion-weighted imaging of the liver: usefulness of ADC values in the differential diagnosis of focal lesions and effect of ROI methods on ADC measurements. MAGMA 2013;26(3):303–312.
10. Vallejo Desviat P, Martínez De Vega V, Recio Rodríguez M, Jiménez De La Peña M, Carrascoso Arranz J. Diffusion MRI in the study of hepatic lesions [in Spanish]. Cir Esp 2013;91(1):9–16.
11. Cui Y, Zhang XP, Sun YS, Tang L, Shen L. Apparent diffusion coefficient: potential imaging biomarker for prediction and early detection of response to chemotherapy in hepatic metastases. Radiology 2008;248(3):894–900.
12. Koh DM, Scurr E, Collins D, et al. Predicting response of colorectal hepatic metastasis: value of pretreatment apparent diffusion coefficients. AJR Am J Roentgenol 2007;188(4):1001–1008.
13. Dietrich O, Heiland S, Sartor K. Noise correction for the exact determination of apparent diffusion coefficients at low SNR. Magn Reson Med 2001;45(3):448–453.
14. Mazaheri Y, Do RK, Shukla-Dave A, Deasy JO, Lu Y, Akin O. Motion correction of multi-b-value diffusion-weighted imaging in the liver. Acad Radiol 2012;19(12):1573–1580.
15. Kandpal H, Sharma R, Madhusudhan KS, Kapoor KS. Respiratory-triggered versus breath-hold diffusion-weighted MRI of liver lesions: comparison of image quality and apparent diffusion coefficient values. AJR Am J Roentgenol 2009;192(4):915–922.
16. Taouli B, Sandberg A, Stemmer A, et al. Diffusion-weighted imaging of the liver: comparison of navigator triggered and breathhold acquisitions. J Magn Reson Imaging 2009;30(3):561–568.
17. Kwee TC, Takahara T, Koh DM, Nievelstein RA, Luijten PR. Comparison and reproducibility of ADC measurements in breathhold, respiratory triggered, and free-breathing diffusion-weighted MR imaging of the liver. J Magn Reson Imaging 2008;28(5):1141–1148.
18. Holzapfel K, Bruegel M, Eiber M, et al. Characterization of small (≤10 mm) focal liver lesions: value of respiratory-triggered echo-planar diffusion-weighted MR imaging. Eur J Radiol 2010;76(1):89–95.
19. Kim SY, Lee SS, Byun JH, et al. Malignant hepatic tumors: short-term reproducibility of apparent diffusion coefficients with breath-hold and respiratory-triggered diffusion-weighted MR imaging. Radiology 2010;255(3):815–823.
20. Jerome NP, Orton MR, d'Arcy JA, Collins DJ, Koh DM, Leach MO. Comparison of free-breathing with navigator-controlled acquisition regimes in abdominal diffusion-weighted magnetic resonance images: effect on ADC

and IVIM statistics. J Magn Reson Imaging doi: 10.1002/jmri24140. Published online April 11, 2013. Accessed April 25, 2013.

21. Bruegel M, Holzapfel K, Gaa J, et al. Characterization of focal liver lesions by ADC measurements using a respiratory triggered diffusion-weighted single-shot echo-planar MR imaging technique. Eur Radiol 2008;18(3):477–485.

22. Shrout PE, Fleiss JL. Intraclass correlations: uses in assessing rater reliability. Psychol Bull 1979;86(2):420–428.

23. Büsing KA, Kilian AK, Schaible T, Debus A, Weiss C, Neff KW. Reliability and validity of MR image lung volume measurement in fetuses with congenital diaphragmatic hernia and in vitro lung models. Radiology 2008;246(2):553–561.

24. Bland JM, Altman DG. Statistical methods for assessing agreement between two methods of clinical measurement. Lancet 1986;1(8476):307–310.

25. Larsen NE, Haack S, Larsen LP, Pedersen EM. Quantitative liver ADC measurements using diffusion-weighted MRI at 3 Tesla: evaluation of reproducibility and perfusion dependence using different techniques for respiratory compensation. MAGMA 2013;26(5):431–442.

26. Kwee TC, Takahara T, Niwa T, et al. Influence of cardiac motion on diffusion-weighted magnetic resonance imaging of the liver. MAGMA 2009;22(5):319–325.

27. Mürtz P, Flacke S, Träber F, van den Brink JS, Gieseke J, Schild HH. Abdomen: diffusion-weighted MR imaging with pulse-triggered single-shot sequences. Radiology 2002;224(1):258–264.

28. Nasu K, Kuroki Y, Fujii H, Minami M. Hepatic pseudo-anisotropy: a specific artifact in hepatic diffusion-weighted images obtained with respiratory triggering. MAGMA 2007;20(4):205–211.

29. Kim SY, Lee SS, Park B, et al. Reproducibility of measurement of apparent diffusion coefficients of malignant hepatic tumors: effect of DWI techniques and calculation methods. J Magn Reson Imaging 2012;36(5):1131–1138.